

See discussions, stats, and author profiles for this publication at: <https://www.researchgate.net/publication/261996714>

Production of Nitrous Oxide From Anaerobic Digester Centrate and Its Use as a Co-oxidant of Biogas to Enhance Energy Recovery

ARTICLE *in* ENVIRONMENTAL SCIENCE & TECHNOLOGY · APRIL 2014

Impact Factor: 5.33 · DOI: 10.1021/es501009j · Source: PubMed

CITATIONS

5

READS

89

3 AUTHORS, INCLUDING:



[Yaniv D. Scherson](#)

Stanford University

10 PUBLICATIONS 53 CITATIONS

SEE PROFILE



[Craig S Criddle](#)

Stanford University

187 PUBLICATIONS 8,506 CITATIONS

SEE PROFILE

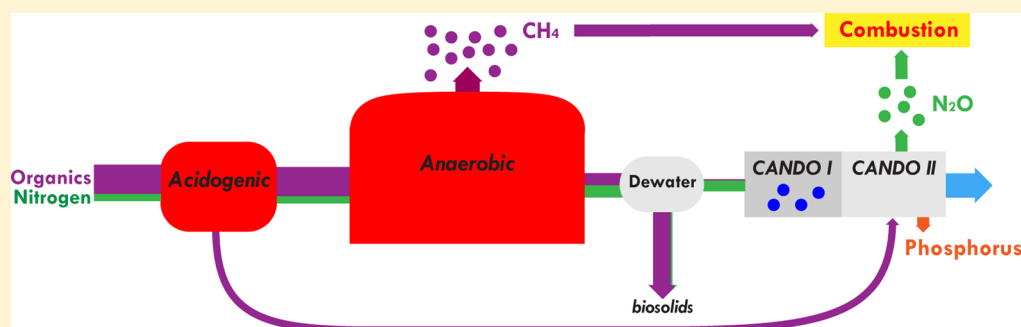
Production of Nitrous Oxide From Anaerobic Digester Centrate and Its Use as a Co-oxidant of Biogas to Enhance Energy Recovery

Yaniv D. Scherson,^{*,†,‡} Sung-Geun Woo,[†] and Craig S. Criddle^{†,‡}

[†]Stanford University, Stanford, California 94305-4020, United States

[‡]NSF Engineering Research Center ReNUWIt, Woods Institute for the Environment, Department of Civil and Environmental Engineering, Stanford University, Stanford, California 94305-4020, United States

S Supporting Information



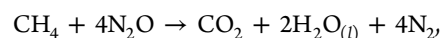
ABSTRACT: Coupled Aerobic-anoxic Nitrous Decomposition Operation (CANDO) is a new process for wastewater treatment that removes nitrogen from wastewater and recovers energy from the nitrogen in three steps: (1) NH_4^+ oxidation to NO_2^- ; (2) NO_2^- reduction to N_2O gas; and (3) N_2O conversion to N_2 with energy production. In this work, we optimize Steps 1 and 2 for anaerobic digester centrate, and we evaluate Step 3 for a full-scale biogas-fed internal combustion engine. Using a continuous stirred reactor coupled to a bench-scale sequencing batch reactor, we observed sustained partial oxidation of NH_4^+ to NO_2^- and sustained (3 months) partial reduction of NO_2^- to N_2O (75–80% conversion, mass basis), with >95% nitrogen removal (Step 2). Alternating pulses of acetate and NO_2^- selected for *Comamonas* (38%), *Ciceribacter* (16%), and *Clostridium* (11%). Some species stored polyhydroxybutyrate (PHB) and coupled oxidation of PHB to reduction of NO_2^- to N_2O . Some species also stored phosphorus as polyphosphate granules. Injections of N_2O into a biogas-fed engine at flow rates simulating a full-scale system increased power output by 5.7–7.3%. The results underscore the need for more detailed assessment of bioreactor community ecology and justify pilot- and full-scale testing.

INTRODUCTION

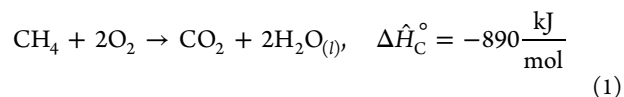
Nitrous oxide (N_2O) is used as a monopropellant in rockets^{1,2} and a power booster oxidant in race cars.^{3,4} In wastewater treatment, however, it is typically considered an unwanted byproduct due to its powerful greenhouse gas warming potential (310 times greater than CO_2).⁵ Consequently, most environmental research has focused on minimizing its production.^{6,7} Maximizing its production, capture, and use for energy generation is a new concept, but is gaining traction, as evidenced by a recent Water Environment Research Federation report recognizing N_2O as a potential renewable energy source.⁸

Energy recovery from wastewater is commonly achieved through anaerobic digestion. Organic matter is converted to CH_4 , and the CH_4 recovered is combusted with oxygen in air to produce energy as electricity and heat. The combustion step destroys CH_4 , a greenhouse gas 21 times more powerful than CO_2 ,⁵ and produces CO_2 (for accounting purposes, this CO_2 is considered greenhouse-gas neutral because of its recent biological origin through photosynthesis). N_2O is like CH_4 :

both are harmful greenhouse gases if released to the atmosphere, and both can be sources of renewable energy if collected and combusted. In fact, N_2O is a more powerful oxidant than O_2 and can increase energy recovery from the combustion of CH_4 : stoichiometric combustion of 1 mol of CH_4 with N_2O releases roughly 30% more energy than stoichiometric combustion of 1 mol of CH_4 with O_2 (eq 1).



$$\Delta\hat{H}_C^\circ = -1219 \frac{\text{kJ}}{\text{mol}}$$



Received: February 27, 2014

Revised: April 28, 2014

Accepted: April 29, 2014

Published: April 29, 2014

Equation 1 shows the heat of combustion ($\Delta\hat{H}_C^\circ$) for CH_4 oxidation with N_2O compared to CH_4 oxidation with O_2 . Combustion with N_2O eliminates the greenhouse gas consequences resulting from its release to the atmosphere.

We previously introduced a new nitrogen treatment process, termed the **Coupled Aerobic-anoxic Nitrous Decomposition Operation (CANDO)**, to remove and recover energy from NH_4^+ nitrogen in wastewater.⁹ The process typically entails three steps: (1) partial aerobic nitrification of NH_4^+ to NO_2^- ; (2) partial heterotrophic denitrification of NO_2^- to N_2O ; and, (3) N_2O conversion to N_2 where energy production is achieved using N_2O as a co-oxidant in CH_4 combustion. Step 2, partial denitrification to N_2O , is novel. Step 1, partial nitrification, is well established at full-scale by the SHARON process;^{10,11} and Step 3, the use of N_2O as an energy source, is commonly exploited in the propulsion and automotive fields.

In a prior study introducing CANDO, we demonstrated Steps 1 and 2 with synthetic wastewater at the bench-scale, achieving 85% conversion of NH_4^+ to NO_2^- (Step 1) and 60–65% conversion of NO_2^- to N_2O (Step 2). We found that alternating pulses of acetate and NO_2^- selected for microorganisms that store acetate as polyhydroxybutyrate (PHB); during an anoxic period with nitrite addition, consumption of PHB was concomitant with reduction of NO_2^- to N_2O . Here, we demonstrate Steps 1 and 2 at the bench-scale with anaerobic digester centrate from a full-scale anaerobic digester at a wastewater treatment plant. We also demonstrate Step 3 with N_2O gas injections into a full-scale biogas-fed internal combustion engine at flow rates expected for full-scale implementation. Anaerobic digester centrate was supplied to an aerobic nitrification bioreactor with 95% conversion of NH_4^+ to NO_2^- (Step 1). The resulting nitrite-rich solution was transferred to a partial-denitrifying bioreactor and reduced to N_2O (Step 2) with 75–80% conversion, with the remainder presumably assimilated, and >95% overall nitrogen removal. N_2O gas injections into a biogas-fed engine (Step 3) increased power output by 5.7–7.3%, as expected.

MATERIALS AND METHODS

CANDO I: Partial Nitrifying Bioreactor (NH_4^+ to NO_2^-).

A five-liter continuous flow bioreactor was used for partial oxidation of NH_4^+ to NO_2^- under the following conditions: $\text{DO} = 0.2 \text{ mg-O}_2/\text{L}$, $T = 35^\circ\text{C}$, $\text{HRT} = 2 \text{ days}$, mixing speed = 200 rpm, $\text{pH} = 7.1$, no solids recycling. The pH was controlled by automated addition of sodium hydroxide solution (0.1M). The reactor was seeded with 100 mL of activated sludge from the Delta Diablo Sanitation District (DDSD) in Antioch, CA and fed centrate from the plant's full-scale anaerobic digester ($\sim 1500 \text{ mg-N L}^{-1} \text{ NH}_4^+$, $1300 \text{ mg-COD L}^{-1}$, $56 \text{ mg-P L}^{-1} \text{ PO}_4^{3-}$, $5200 \text{ mg-CaCO}_3 \text{ L}^{-1}$, $\text{pH} = 8.6$). The reactor was operated in start-up mode for 2 months followed by a 6-month period of stable operation. During start-up, HRT was slowly adjusted from 8 to 2 days. Operation was stable when at least 90% of the influent NH_4^+ converted to NO_2^- and fluctuations in the concentration of the nitrogen species did not change by more than 10%. The reactor achieved a maximum loading rate of $5.2 \text{ kg-N m}^{-3} \text{ d}^{-1}$. The reactor effluent was the influent for a partial denitrifying bioreactor, providing NO_2^- for partial denitrification.

CANDO II: Partial Denitrifying Bioreactor (NO_2^- to N_2O). A four-liter partial denitrifying sequencing batch reactor (SBR) was operated for 6 months (3 months of start-up and optimization followed by 3 months of stable operation).

Acetate was supplied as electron donor, and NO_2^- present in the effluent of the partial nitrifying bioreactor was the electron acceptor. The reactor was inoculated with N_2O -producing biomass from a previous study.⁹ Previously, the inoculum had adapted to synthetic wastewater then to anaerobic digester centrate from the Sunnyvale Water Pollution Control Plant. Reactor operation was adjusted to maximize conversion of NO_2^- to N_2O and removal of NO_2^- from solution. Optimal performance was achieved through four phases of operation in a 48-h cycle (Figure 1): (1) anaerobic phase (24 h) in which

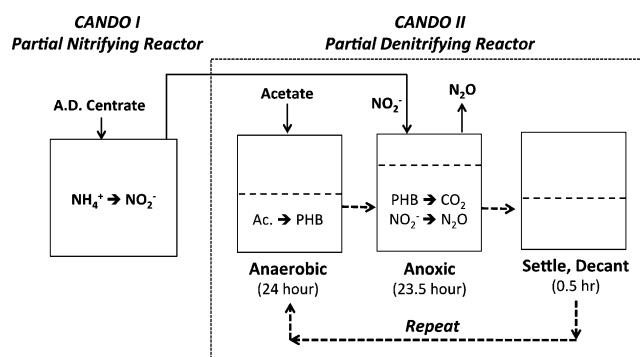


Figure 1. Operation of N_2O producing sequencing batch reactor.

acetate was added and assimilated as PHB during a fast fill (0.5 h) followed by a react period (23.5 h); (2) anoxic phase (23.5 h), in which nitrite-rich effluent from the partial nitrifying reactor was added for oxidation of PHB coupled to reduction of NO_2^- to N_2O during a fast fill (0.1 h) followed by a react period (23.4 h); (3) settling phase (25 min); and (4) decant phase (5 min). The cycle began with a three-liter working volume. One hundred milliliters of stock sodium acetate solution (122 mM) was added to initiate the Anaerobic phase (initial acetate concentration in the reactor of 4 mM or $\sim 250 \text{ mg COD L}^{-1}$). After completion of the anaerobic phase, 180 mL of liquid from the partial nitrifying reactor ($\sim 1,400 \text{ mg-N L}^{-1} \text{ NO}_2^-$) was added to initiate the anoxic phase (initial NO_2^- -N concentration of 6 mM or $\sim 85 \text{ mg-N L}^{-1}$). The loading rates were $0.25 \text{ kg COD m}^{-3} \text{ day}^{-1}$ and $0.085 \text{ kg-N m}^{-3} \text{ day}^{-1} \text{ NO}_2^-$. Operational parameters were as follows: $T = 21^\circ\text{C}$, $\text{HRT} = 10 \text{ days}$, mixing speed of 150 rpm, $\text{pH} = 7.1$. No biomass was wasted during the study period (3 months).

Bioreactor Monitoring. A helium sweep (100 mL min^{-1}) stripped dissolved N_2O from the partial denitrifying bioreactor. Dissolved N_2O levels, measured with an in situ probe, did not exceed 1% of saturation. The gas stream was sampled every 5 min for analysis on a Varian 3800 Gas Chromatograph equipped with a 6-foot Porapak Q column ($T = 80^\circ\text{C}$), 6-foot 5 Å molecular sieve column, and thermal conductivity detector ($T = 80^\circ\text{C}$). For calibration, a three-point external calibration curve was prepared by serial dilutions of a gas standard containing 500 ppm of N_2O and 500 ppm of N_2 (Scott Specialty Gases).

NO_2^- , NO_3^- , and NH_4^+ were assayed with a Dionex ICS-1600 ion chromatograph using a 4.5 mM sodium carbonate and 1.4 mM sodium bicarbonate eluent, and equipped with ICS-1600 isocratic pump, Orion 9512 ion selective electrode (for NH_4^+), DS6 heated conductivity detector (for NO_2^- , NO_3^-), AS-DV automated sampler, two AG22 50 mm guard columns, two AS22 250 mm ion-exchange columns, ASRS300 2 mm

suppressor, and Thermo Scientific Chromeleon 7 software (version 7.1 SR1).

Total and volatile suspended solids in the partial denitrifying reactor were stable at $\sim 650 \text{ mg L}^{-1}$ and $\sim 200 \text{ mg L}^{-1}$ (Standard Methods¹²) during the study period. Poly-3-hydroxybutyrate (PHB) was assayed by gas chromatography (Agilent 6890N gas chromatograph equipped with an HP-5 column and FID detector), as previously described.¹³

TEM Imaging. Transmission electron microscopy (TEM) images of intracellular granules were acquired using an image aberration-corrected FEI Titan 80–300 environmental (scanning) transmission electron microscope (TEM) operated at 80 kV. Elemental composition of the intracellular granules was obtained using an Oxford SDD Xmax energy dispersive X-ray spectrometer operated at 80 kV in TEM mode, and by focusing the electron beam to $0.2 \mu\text{m}$ (granule only) and $1 \mu\text{m}$ (cell cytoplasm) diameter areas.

DNA Extraction, PCR, Cloning and Sequencing of N_2O Producing Biomass. Biomass was sampled from the partial denitrifying bioreactor at the beginning (inoculum) and end of the monitoring period. Genomic DNA (gDNA) from the inoculum and the reactor biomass was extracted using the FastDNA Spin Kit for Soil (MP Biomedicals, Solon, OH) per the manufacturer's instruction. Near complete 16S rRNA gene sequences ($\sim 1450 \text{ bp}$) were amplified from extracted gDNA samples using the primer set 8F (5'-AGAGTTTGATCCTGG-CTCAG-3') and 1492R (5'-GGTTACCTTGTTACGACTT-3'). The PCR reaction was carried out with a $25\text{-}\mu\text{L}$ mixture containing $0.4 \mu\text{M}$ of each primer, 1X Fail-Safe PCR buffer F (Epicentre, Madison, WI), 1.25 units of AmpliTaq LD Taq Polymerase (Applied Biosystems, Foster City, CA), and 20–30 ng of genomic DNA template. The PCR thermocycling steps were: (i) 94°C for 5 min; (ii) 35 cycles of 94°C for 45 s, 55°C for 30 s, 72°C for 90 s, and (iii) an extension at 72°C for 10 min. The PCR product was verified using 1.5% agarose gel electrophoresis and purified via the PureLink Quick PCR purification Kit (Invitrogen, Carlsbad, CA). Cloning and sequencing was performed as previously described.¹⁴ Primer 8F (5'-AGAGTTTGATCCTGGCTCAG-3') was used for the reactor biomass, and primer 1492R (5'-GGTTACCTTGTTACGACTT-3') was used for the inoculum. All together, 127 sequences were obtained from the inoculum, and 135 sequences were obtained from the reactor biomass. Putative chimeric sequences were removed using BELLEROPHON,¹⁵ including 33 in the inoculum and 38 in the reactor biomass. The remaining 94 sequences from the inoculum and 97 from the reactor biomass were identified using EzTaxon-e server¹⁶ and 16S rRNA sequence data. Sequences reported as "uncultured clones" are less than 90% similar to the most closely related species in EzTaxon-e and most closely match "uncultured clones" in GenBank.

N_2O Injections into Biogas-Fed Engines. The effects of using N_2O as a biogas co-oxidant with oxygen in air was evaluated in a full-scale biogas-fed internal combustion engine (7040 in³ Waukesha V-12) at the South Bayside System Authority in Redwood City, CA. Under normal operating conditions (i.e., "baseline conditions"), this engine combusts $1650 \text{ L}^3 \text{ min}^{-1}$ biogas (59% CH_4) with oxygen in air to maintain 1000 rpm. The carburetor sets the air flow rate (not measured) for a given biogas flow rate to maintain slightly lean combustion ($\sim 0.5\%$ excess O_2 in the exhaust). In order to increase power output with N_2O , N_2O was used to replace O_2 as oxidant, but the ratio of biogas to air could not be altered

due to limitations in allowed adjustments to the carburetor. Accordingly, N_2O was supplied together with additional biogas such that the combined flow rate was roughly one-hundredth that of the baseline biogas and air volumetric flow (Supporting Information, SI, Figure S1). Mixtures of N_2O and biogas were injected through a gas spray nozzle (Nitrous Express, Texas) at the fuel/oxidant-intake manifold located immediately upstream of the piston chamber, and downstream of the carburetor. Eight injection experiments were conducted where the flow rate of N_2O was fixed ($0.2 \text{ kg N}_2\text{O min}^{-1}$, $100 \text{ L}^3 \text{ min}^{-1}$), and, the flow rate of additional biogas varied ($4.0, 4.6, 5.6, 6.4, 9.0, 10.8, 12.2$, and $14.6 \text{ L}^3 \text{ min}^{-1}$) resulting in gas mixtures that were all lean, but had increasingly rich molar oxidizer (N_2O) to fuel (CH_4) ratios (O/F): 41, 37, 30, 26, 19, 16, 14, and 11. Stoichiometric $\text{CH}_4/\text{N}_2\text{O}$ combustion occurs at O/F = 4 (eq 1). For each injection, gas phase N_2O was drawn from the headspace of a K-cylinder (750 psi), and additional biogas was drawn from the engine fuel supply line (5 psi). In-line orifices of varying diameter ($0.019\text{--}0.038 \text{ in.}$) regulated gas flow rate, and a solenoid valve activated flow. Total biogas flow to the engine decreased slightly (up to 10%) with each injection because the supply of biogas and N_2O decreased pressure immediately downstream of the carburetor. Increases in power output associated with N_2O addition were therefore measured as the change in RPM/biogas-flow ratio compared to baseline operation (no N_2O injection).

RESULTS AND DISCUSSION

Bioreactor Performance: NH_4^+ to NO_2^- to N_2O . The partial nitrifying reactor (CANDO I) community achieved efficient conversion of NH_4^+ to NO_2^- (95% conversion) by applying conditions (low DO, high temperature, 2-day HRT) that selected against nitrite-oxidizing bacteria. Typical concentrations in the reactor were: $90 \text{ mg-N L}^{-1} \text{ NH}_4^+$ (SD = 60 mg-N L^{-1}); $1400 \text{ mg-N L}^{-1} \text{ NO}_2^-$ (SD = 130 mg-N L^{-1}); $50 \text{ mg-N L}^{-1} \text{ NO}_3^-$ (SD = 20 mg-N L^{-1}). The effluent from this reactor contained the nitrite required as electron acceptor for the partial denitrifying (N_2O -producing) bioreactor.

The partial denitrifying bioreactor (CANDO II) achieved efficient conversion of NO_2^- to N_2O (Table 1) and a high

Table 1. Conversion of Ammonium to Nitrite (%) and % Removal of Nitrogen Species^a

	partial nitrification (CANDO I)	partial denitrification (CANDO II)		combined (CANDO I & II)	
	% NH_4^+ to NO_2^-	% NO_2^- to N_2O	% N removed	% NH_4^+ to N_2O	% N removed
%	95	78	96	74	98
SD	5	5	2	5	<1

^aThe study period included 45 cycles. Of these cycles, 8 were monitored for initial and final nitrite concentration and N_2O production. An additional 32 cycles were monitored for N_2O production only with highly reproducible patterns.

fraction of NO_2^- removal. This was achieved by supplying acetate and NO_2^- at a COD/N ratio of 3 (COD/N is 1.14 for reduction of NO_2^- to N_2O without cell synthesis). At higher COD/N ratios, not all of the acetate was incorporated into biomass during the anaerobic phase, and oxidation of the residual acetate drove denitrification to N_2 . At lower COD/N ratios, insufficient acetate was converted into PHB in the anaerobic phase, and the PHB was insufficient for reduction of

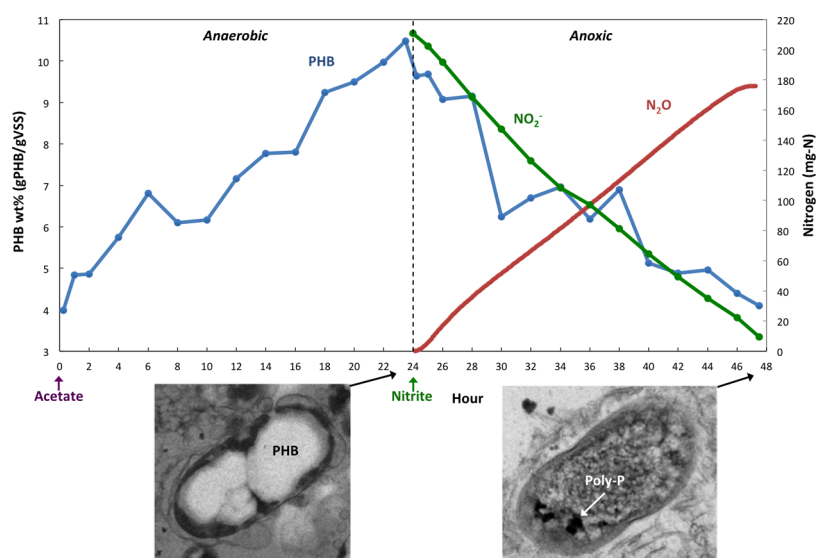


Figure 2. Cycle 45: changes in PHB, NO_2^- , and N_2O . Intracellular PHB granules shown at end of anaerobic period (24 h), and intracellular granules containing high phosphorus levels (possibly Poly-P) shown at end of anoxic period (48 h).

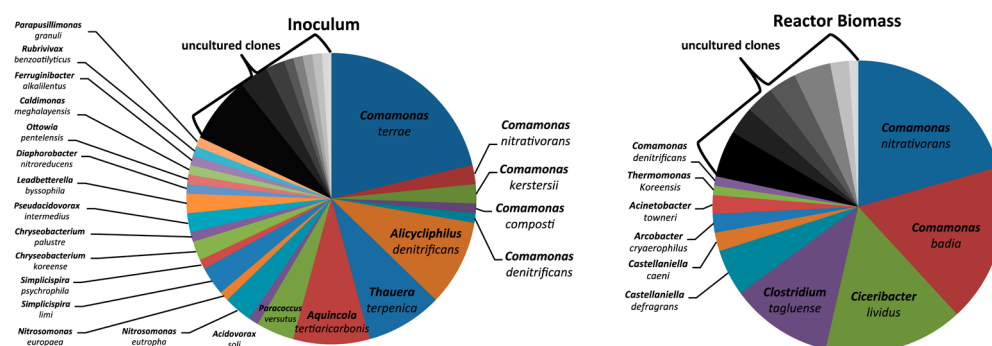


Figure 3. Species detected in 16S rRNA clone libraries prepared for the bioreactor community at beginning of the study period (Day 0) and the end of the study period (Day 90).

nitrite; residual NO_2^- remained in solution at the end of the anoxic phase.

Table 1 summarizes average efficiencies for conversion of NH_4^+ to NO_2^- in the partial nitrifying reactor, for conversion of NO_2^- to N_2O in the partial denitrifying reactor, and for overall nitrogen removal from the water phase. Conversion and removal percentages are reported on a nitrogen mass basis. Addition of nitrite at the beginning of the anoxic phase resulted in an initial NO_2^- concentration of 75–85 mg-N L^{-1} . Removal of NO_2^- was essentially complete within 24 h. Most cycles achieved 75–85% conversion of NO_2^- to N_2O , with >95% removal of nitrogen from the aqueous phase. Combining Steps 1 and 2, the two reactors achieved 74% conversion of NH_4^+ to N_2O and 98% removal of influent dissolved nitrogen.

Figure 2 illustrates changes in PHB, NO_2^- , and N_2O over a single cycle and TEM images of intracellular granules at the end of the anaerobic and anoxic phases. Acetate consumption at the beginning of the anaerobic phase correlated with an increase in intracellular PHB accumulation. Nitrite addition at the beginning of the anoxic phase correlated with a decrease in intracellular PHB, indicating that PHB oxidation was the likely source of reducing equivalents for nitrite reduction to N_2O . For this cycle, 80% of the NO_2^- converted to N_2O ; the remainder was presumably assimilated. TEM images show intracellular PHB granules at the end of the anaerobic phase (24 h), and

intracellular poly phosphate (Poly-P) granules, at the end of the anoxic phase (48 h). TEM elemental analyses indicated that the phosphorus content of the polyphosphate granules was six times that of the cytoplasm. The PHB granules contained no detectable phosphorus (SI Table S1). The phosphorus (P) content of the biomass at the end of the anoxic phase was 2.7% DW. P content is typically 1.5–2% for activated sludge biomass and 4–5% for biomass from enhanced biological phosphorus removal (EBPR) systems.¹⁷

Throughout the study, volatile suspended solids remained stable at 200 mg VSS L^{-1} for the partial denitrifying reactor. The average specific N_2O production rate was 900 $\mu\text{mol-N}_2\text{O}$ per g VSS per h. This is higher than our previously reported value of 200 $\mu\text{mol N}_2\text{O}$ per g VSS per h⁹ for synthetic feed and other published values that range from 200 $\mu\text{mol N}_2\text{O}$ per g VSS per h¹⁸ to 500 $\mu\text{mol N}_2\text{O}$ per g VSS per h.¹⁹

Microbial Ecology. Figure 3 compares the species-level community composition for the partial denitrifying bioreactor at the beginning and end of the monitoring period. *Comamonas* were the most abundant genus. When study period began, the dominant genera were *Comamonas* (28%), *Alicyclophilus* (10%), *Thauera* (9%), *Aquicola* (9%), and *Paracoccus* (4%). When the study period ended, the dominant community members were *Comamonas* (38%), *Ciceribacter* (16%), and *Clostridium* (11%) (see SI Table S2 for best-matched type strain). Within the

Comamonas genus, two species dominated: *Comamonas nitrivorans* and *Comamonas badia*. Previous reports indicate that species of the *Comamonas* genus produce N_2O under anoxic conditions,^{20,21} accumulate PHB,^{22–25} and assimilate phosphorus as Poly-P.²⁶ A notable minor community member was *Acinetobacter* (2%), a species implicated in phosphorus uptake as Poly-P.^{27–29}

Biogas Combustion with N_2O . Figure 4 illustrates increases in power output in a full-scale biogas-fed internal

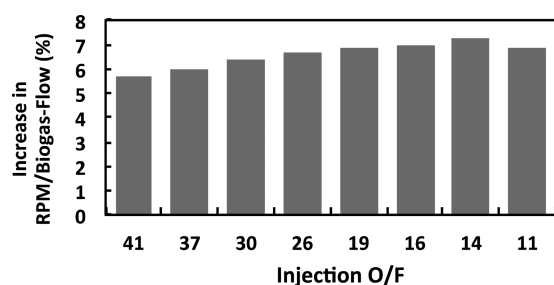


Figure 4. Changes in RPM/biogas-flow as a function of the O/F ratio of the $\text{N}_2\text{O}/\text{CH}_4$ injection in full-scale biogas-fed engine. The ratio of RPM/Biogas-flow with N_2O injection is reported as a percent increase from the ratio of RPM/Biogas-flow without N_2O injection.

combustion engine as a function of the molar O/F ratio of the N_2O and biogas injection. Stoichiometric combustion of CH_4 and N_2O occurs at O/F = 4 (molar basis): mixtures with more N_2O (excess oxidant) are “lean”, whereas mixtures with less N_2O (excess fuel) are “rich”. For this study, all injections were lean. Injections that were increasingly rich (O/F ratio closer to stoichiometric combustion) resulted in greater gains in the RPM/biogas-flow ratio. The leanest injection (O/F = 41)

increased RPM/biogas-flow by 5.7%, whereas the least lean injection (O/F = 14) increased RPM/biogas-flow by 7.3%. An even leaner injection (O/F = 11) decreased power output slightly, likely due to uneven distribution of the injection gas mixture. Better control of the O/F ratio through direct piston injection and control of the bulk biogas and airflow would mitigate this effect, but was not practical for this study.

The NO_x emissions and exhaust gas temperatures were greater for injections that were closer to stoichiometric combustion: the injection with O/F = 41 resulted in 1450 ppm of NO_x in the exhaust gas and the lowest exhaust temperature, whereas the injection with O/F = 14 resulted in 1640 ppm of NO_x in the exhaust gas and the highest exhaust temperature (SI Figure S2). NO_x emissions are caused by the recombination of oxygen (O) and nitrogen (N) radicals that generally originate from gaseous oxygen (O_2) and nitrogen (N_2). Recombination of O and N radicals increases at elevated temperatures (>1600 °C) and short gas residence times: when combustion temperatures are high, more NO_x forms.³⁰ Many biogas combustion engines operate lean to lower the combustion temperature and decrease NO_x emissions. The consequence is that the power output decreases as compared to the maximum power output that occurs with stoichiometric combustion. NO_x emissions were higher than most discharge limits. This was expected because we had limited capacity to modify the engine or its operating conditions. Injections of N_2O without adjustments to the carburetor increase combustion temperature compared to baseline operation with air alone as oxidant. Operation at an elevated temperature increases NO_x formation from N_2O and from air. Lower NO_x emissions are expected to result from lean combustion, direct injection into each piston ensuring a more uniform combustion

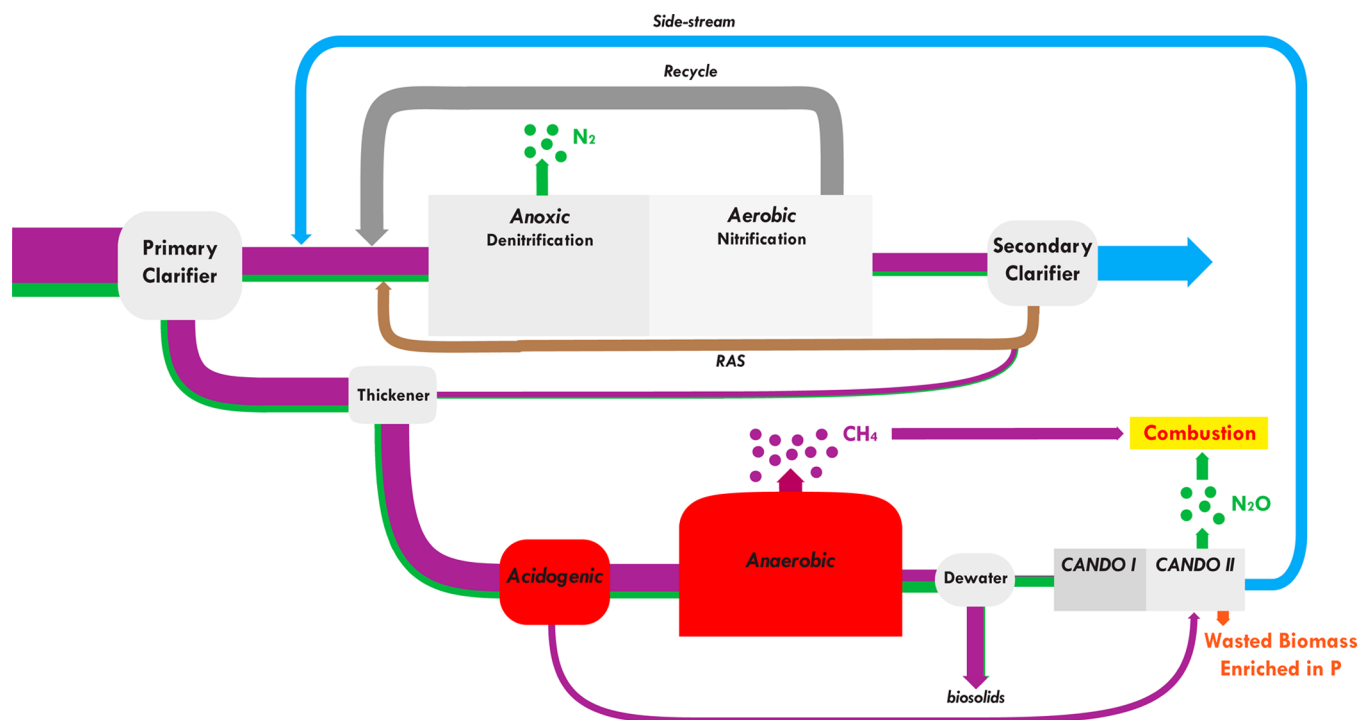


Figure 5. Potential wastewater treatment configuration that uses CANDO to remove nitrogen from the side-stream. Flows of bCOD to methane are shown in purple; flows of nitrogen to N_2O and N_2 are shown in green. Line width is proportional to mass flux. Biogas combustion with N_2O increases energy production. The potential for P removal is also shown.

mixture, adjustments to timing of gas injections into the piston, and decreased combustion temperature.

In this study we used pure N_2O to simulate N_2O produced from a full-scale CANDO system. In practice, N_2O will be recovered with gas impurities similar to those found in biogas (e.g., CO_2 and H_2O). We note, however, that the N_2O stream, and any associated gas impurities, is expected to be small relative to the biogas stream from an anaerobic digester. Moreover, processes currently used to remove impurities from biogas prior to combustion will also remove impurities from a biogas stream amended with gases recovered from CANDO.

Figure 5 shows a hypothetical treatment configuration in which CANDO is used to remove nitrogen from the side-stream (anaerobic digester centrate) as N_2O . Conventional nitrification–denitrification is used to remove biodegradable COD (bCOD) and nitrogen in the mainstream. Anaerobic digestion of settled solids is used to produce biogas methane that is combusted with O_2 in air and N_2O as co-oxidant. In this study, we used helium to remove dissolved N_2O . In practice, air or biogas could be used for gas stripping or a vacuum applied. Side-stream treatment with CANDO, or other side-stream treatment processes, reduces the nitrogen load on the mainstream, decreasing demand for bCOD for denitrification. Primary clarifiers can therefore operate more efficiently: more of the influent bCOD can be diverted to anaerobic digestion for biogas production, with enough bCOD still remaining in the primary effluent to enable mainstream denitrification. Diversion of more primary solids to anaerobic digestion enables more production of methane. It also results in fewer biosolids for disposal compared to aerobically generated secondary solids because primary solids are more biodegradable. Unlike other processes that remove side-stream nitrogen, additional energy is recovered through biogas combustion with N_2O .

CANDO uses an anaerobic-anoxic cycle that it is similar to processes used for EBPR. In EBPR systems, anaerobic and aerobic cycling selects for organism that store endogenous carbon as polyhydroxyalkanoates (PHAs such as PHB) and glycogen. Phosphorus-accumulating organisms produce polyphosphate during aerobic oxidation of PHAs. In CANDO, however, polyphosphate is accumulated during the anoxic phase.

CANDO is expected to decrease oxygen requirements and decrease biomass production compared to conventional nitrification–denitrification. An alternative is the CANON process using Anammox bacteria.⁹ Over 100 full-scale Anammox systems exist today with reportedly efficient and stable operation.^{31,32} This process is somewhat more attractive from the standpoint of energy savings and biomass production, but Anammox bacteria grow slowly,³³ and there are concerns about process stability^{34,35} and the effects of inhibitors, including dissolved oxygen, heavy metals, sulfide, salt, free ammonium, free nitrous acid, pharmaceuticals, and toxic organics.^{34–45} CANDO is likely to be stable and resistant to upsets: *Comamonas*, the major community members, are fast growing, adaptable,⁴⁶ and implicated in the degradation of many toxic compounds including steroids,⁴⁷ testosterone,⁴⁶ and aromatic compounds such as nitrobenzene,^{48–50} 4-chloronitrobenzene,⁵⁰ 3-chloroaniline,⁵¹ phenanthrene, naphthalene, and anthracene.⁵² Fast growth rates enable shorter residence times and more rapid recovery from upsets. Formation of polyphosphate granules suggests a potential for phosphorus recovery. Pilot-scale studies are needed to evaluate these potential benefits at a commercially relevant scale. In addition, a

holistic analysis of energy and nutrient inputs and outputs is needed to enable comparison of different treatment configurations.

■ ASSOCIATED CONTENT

Supporting Information

Side-view schematic of the setup for the N_2O injections into the biogas-fed engine. The reported oxidizer to fuel ratio (O/F) is the molar ratio between the added N_2O and added biogas (Figure S1); phosphorus content (as wt %) in granules and cytoplasm (Table S1); and dominant bacterial species populations (>10 % relative abundance) and best-matched type strains based on partial 16S rRNA (~1000 bp) (Table S2); increases in NO_x emissions as a function of injection O/F (Figure S2). This material is available free of charge via the Internet at <http://pubs.acs.org>.

■ AUTHOR INFORMATION

Corresponding Author

*Phone: (650) 736-2274; e-mail: yaniv@stanford.edu.

Notes

The authors declare no competing financial interest.

■ ACKNOWLEDGMENTS

Support for this work was provided in part by the U.S. National Science Foundation Engineering Research Center Reinventing the Nation's Urban Water Infrastructure (ReNUWIt) (Award No. EEC-1028968), the Woods Institute for the Environment at Stanford University, a gift from Veolia Water, and a grant from the U.S. National Science Foundation Partnership for Innovation Research Technology Translation Program (Award No. 109802). We are extremely grateful to the Delta Diablo Sanitation District for critical financial, operational, and monitoring support of our bench-scale system, and the South Bayside System Authority for support with biogas engine testing. We thank Darrel Cain, Bill Svoboda, Gurmukh Grewal, Jason Wong, Amanda Roa, Peter Kistenmacher, Keith Jenne, Mick Daly, and Chuck Fenton.

■ REFERENCES

- (1) Scherson, Y. D.; Lohner, K. A.; Cantwell, B.; Kenny, T. Small-Scale Planar Nitrous Oxide Monopropellant Thruster for "Green" Propulsion and Power Generation. In *46th AIAA/ASME/SAE/ASEE Joint Propulsion Conference & Exhibit*; American Institute of Aeronautics and Astronautics: Nashville, TN, 2010; pp 1–9.
- (2) Scherson, Y.; Lohner, K.; Lariviere, B.; Cantwell, B.; Kenny, T. A Monopropellant Gas Generator Based on N_2O Decomposition for "Green" Propulsion and Power Applications. In *45th AIAA/ASME/SAE/ASEE Joint Propulsion Conference & Exhibit*; American Institute of Aeronautics and Astronautics: Denver, CO, 2009; pp 1–9.
- (3) Pfahl, U.; Ross, M.; Shepherd, J.; Pasamehmetoglu, K.; Unal, C. Flammability limits, ignition energy, and flame speeds in H_2 – CH_4 – NH_3 – N_2O – O_2 – N_2 mixtures. *Combust. Flame* **2000**, *123*, 140–158.
- (4) Tsang, W.; Herron, J. T. Chemical kinetic data base for propellant combustion I. Reactions involving NO , NO_2 , HNO , HNO_2 , HCN and N_2O . *J. Phys. Chem. Ref. Data* **1991**, *20*, 609.
- (5) U.S. EPA Office of Atmospheric Programs Climate Change Division. Global Anthropogenic Non- CO_2 Greenhouse Gas Emissions: 1990–2020; Washington, DC, 2006.
- (6) Kampschreur, M. J.; Temmink, H.; Kleerebezem, R.; Jetten, M. S. M.; van Loosdrecht, M. C. M. Nitrous Oxide emission during wastewater treatment. *Water Res.* **2009**, *43*, 4093–4103.
- (7) Ahn, J. H.; Kim, S.; Park, H.; Rahm, B.; Pagilla, K.; Chandran, K. N_2O Emissions from activated sludge processes, 2008–2009: Results

of a national monitoring survey in the United States. *Environ. Sci. Technol.* **2010**, *44*, 4505–4511.

(8) WERF. Energy Production and Efficiency Research—The Roadmap to Net-Zero Energy; Alexandria, VA, 2011; pp 1–8.

(9) Scherson, Y. D.; Wells, G. F.; Woo, S.-G.; Lee, J.; Park, J.; Cantwell, B. J.; Criddle, C. S. Nitrogen removal with energy recovery through N_2O decomposition. *Energy Environ. Sci.* **2013**, *6*, 241–248.

(10) Mulder, J. W.; van Loosdrecht, M. C. M.; Hellinga, C.; van Kempen, R. Full-scale application of the SHARON process for treatment of rejection water of digested sludge dewatering. *Water Sci. Technol.* **2001**, *44*, 127–134.

(11) Mulder, J. W.; Duin, J. O. J.; Goverde, J.; Poiesz, W. G.; van Veldhuizen, H. M.; van Kempen, R.; Roeleveld, P. Full-scale experience with the SHARON process through the eyes of the operators. In *WEFTEC*; Water Environment Federation, 2006; pp 5256–5270.

(12) *Standard Methods for the Examination of Water and Wastewater*, 20th ed.; American Public Health Association, American Water Works Association, Water Environment Federation: Washington, DC.

(13) Pieja, A. J.; Sundstrom, E. R.; Criddle, C. S. Poly-3-hydroxybutyrate metabolism in the type II methanotroph *Methylocystis Parvus* OBBP. *Appl. Environ. Microbiol.* **2011**, *77*, 6012–6019.

(14) Wells, G. F.; Park, H.-D.; Eggleston, B.; Francis, C. A.; Criddle, C. S. Fine-scale bacterial community dynamics and the taxa–time relationship within a full-scale activated sludge bioreactor. *Water Res.* **2011**, *45*, 5476–5488.

(15) Huber, T.; Faulkner, G.; Hugenholtz, P. Bellerophon: A program to detect chimeric sequences in multiple sequence alignments. *Bioinformatics* **2004**, *20*, 2317–2319.

(16) Kim, O. S.; Cho, Y. J.; Lee, K.; Yoon, S. H.; Kim, M.; Na, H.; Park, S. C.; Jeon, Y. S.; Lee, J. H.; Yi, H.; et al. Introducing EzTaxon-E: A Prokaryotic 16S rRNA gene sequence database with phylotypes that represent uncultured species. *Int. J. Syst. Evol. Microbiol.* **2012**, *62*, 716–721.

(17) Blackall, L. L.; Crocetti, G. R.; Saunders, A. M.; Bond, P. L. A review and update of the microbiology of enhanced biological phosphorus removal in wastewater treatment plants. *Antonie Van Leeuwenhoek* **2002**, *81*, 681–691.

(18) Lemaire, R.; Meyer, R.; Taske, A.; Crocetti, G. R.; Keller, J.; Yuan, Z. Identifying causes for N_2O accumulation in a lab-scale sequencing batch reactor performing simultaneous nitrification, denitrification and phosphorus removal. *J. Biotechnol.* **2006**, *122*, 62–72.

(19) Zeng, R. J.; Yuan, Z.; Keller, J. Enrichment of denitrifying glycogen-accumulating organisms in anaerobic/anoxic activated sludge system. *Biotechnol. Bioeng.* **2003**, *81*, 397–404.

(20) Horiba, Y.; Tabrez Khan, S.; Hiraishi, A. Characterization of the microbial community and culturable denitrifying bacteria in a solid-phase denitrification process using poly (ϵ -caprolactone) as the carbon and energy source. *Microbes Environ.* **2005**, *20*, 25–33.

(21) Etchebehere, C.; Errazquin, M. I.; Dabert, P.; Moletta, R.; Muxí, L. *Comamonas nitrivorans* sp. nov., a novel denitrifier isolated from a denitrifying reactor treating landfill leachate. *Int. J. Syst. Evol. Microbiol.* **2001**, *51*, 977–983.

(22) Thakor, N.; Trivedi, U.; Patel, K. C. Biosynthesis of medium chain length poly(3-hydroxyalkanoates) (mcl-PHAs) by *Comamonas testosteroni* during cultivation on vegetable oils. *Bioresour. Technol.* **2005**, *96*, 1843–1850.

(23) Zakaria, M. R.; Ariffin, H.; Mohd Johar, N. A.; Abd-Aziz, S.; Nishida, H.; Shirai, Y.; Hassan, M. A. Biosynthesis and characterization of poly(3-hydroxybutyrate-co-3-hydroxyvalerate) copolymer from wild-type *Comamonas* sp. EB172. *Polym. Degrad. Stab.* **2010**, *95*, 1382–1386.

(24) Lee, W.-H.; Azizan, M. N. M.; Sudesh, K. Effects of culture conditions on the composition of poly(3-hydroxybutyrate-co-4-hydroxybutyrate) synthesized by *Comamonas acidovorans*. *Polym. Degrad. Stab.* **2004**, *84*, 129–134.

(25) Yee, L.-N. Polyhydroxyalkanoate synthesis by recombinant *Escherichia coli* JM109 expressing PHA biosynthesis genes from

Comamonas sp. EB172. *J. Microb. Biochem. Technol.* **2012**, *04*, 103–110.

(26) Hiraishi, A.; Morishima, Y. Capacity for polyphosphate accumulation of predominant bacteria in activated sludge showing enhanced phosphate removal. *J. Ferment. Bioeng.* **1990**, *69*, 368–371.

(27) Jørgensen, K. S.; Pauli, A. S. Polyphosphate accumulation among denitrifying bacteria in activated sludge. *Anaerobe* **1995**, *1*, 161–168.

(28) Streichan, M.; Golecki, J. R.; Schön, G. Polyphosphate-accumulating bacteria from sewage plants with different processes for biological phosphorus removal. *FEMS Microbiol. Ecol.* **1990**, *73*, 113–124.

(29) Deinema, M. The accumulation of polyphosphate in *Acinetobacter* spp. *FEMS Microbiol. Lett.* **1980**, *9*, 275–279.

(30) US Environmental Protection Agency Office of Air Quality. *Nitrogen Oxides (NO_x), Why and How They Are Controlled*; Research Triangle Park, NC, 1999; p. EPA 456/F-99-006R.

(31) Lackner, S.; Gilbert, E. M.; Vlaeminck, S. E.; Joss, A.; Horn, H.; van Loosdrecht, M. C. M. Full-scale partial nitrification/anammox experiences—An application survey. *Water Res.* **2014**, *55C*, 292–303.

(32) De Clippeleir, H.; Vlaeminck, S. E.; De Wilde, F.; Daeninck, K.; Mosquera, M.; Boeckx, P.; Verstraete, W.; Boon, N. One-stage partial nitrification/anammox at 15 °C on pretreated sewage: Feasibility demonstration at lab-scale. *Appl. Microbiol. Biotechnol.* **2013**, *97*, 10199–10210.

(33) Kartal, B.; Kuenen, J. G.; van Loosdrecht, M. C. . Sewage treatment with anammox. *Science* **2010**, *328*, 702–703.

(34) Joss, A.; Derlon, N.; Cyprien, C.; Burger, S.; Szivak, I.; Traber, J.; Siegrist, H.; Morgenroth, E. Combined nitrification-anammox: Advances in understanding process stability. *Environ. Sci. Technol.* **2011**, *45*, 9735–9742.

(35) Jin, R.-C.; Yang, G.-F.; Yu, J.-J.; Zheng, P. The inhibition of the anammox process: A review. *Chem. Eng. J.* **2012**, *197*, 67–79.

(36) Tang, C.-J.; Zheng, P.; Chai, L.-Y.; Min, X.-B. Thermodynamic and kinetic investigation of anaerobic bioprocesses on ANAMMOX under high organic conditions. *Chem. Eng. J.* **2013**, *230*, 149–157.

(37) Alvarino, T.; Katsou, E.; Malamis, S.; Suarez, S.; Omil, F.; Fatone, F. Inhibition of biomass activity in the via nitrite nitrogen removal processes by veterinary pharmaceuticals. *Bioresour. Technol.* **2014**, *152*, 477–483.

(38) Zhang, Q.-Q.; Chen, H.; Liu, J.-H.; Yang, B.-E.; Ni, W.-M.; Jin, R.-C. The robustness of ANAMMOX process under the transient oxytetracycline (OTC) shock. *Bioresour. Technol.* **2014**, *153*, 39–46.

(39) Jin, R.-C.; Yang, G.-F.; Zhang, Q.-Q.; Ma, C.; Yu, J.-J.; Xing, B.-S. The effect of sulfide inhibition on the anammox process. *Water Res.* **2013**, *47*, 1459–1469.

(40) Yang, G.-F.; Jin, R.-C. The joint inhibitory effects of phenol, copper (II), oxytetracycline (OTC) and sulfide on anammox activity. *Bioresour. Technol.* **2012**, *126*, 187–192.

(41) Aktan, C. K.; Yapsakli, K.; Mertoglu, B. Inhibitory effects of free ammonia on anammox bacteria. *Biodegradation* **2012**, *23*, 751–762.

(42) Carvajal-Arroyo, J. M.; Sun, W.; Sierra-Alvarez, R.; Field, J. A. Inhibition of anaerobic ammonium oxidizing (anammox) enrichment cultures by substrates, metabolites and common wastewater constituents. *Chemosphere* **2013**, *91*, 22–27.

(43) Jensen, M. M.; Thamdrup, B.; Dalsgaard, T. Effects of specific inhibitors on anammox and denitrification in marine sediments. *Appl. Environ. Microbiol.* **2007**, *73*, 3151–3158.

(44) Lotti, T.; van der Star, W. R. L.; Kleerebezem, R.; Lubello, C.; van Loosdrecht, M. C. M. The effect of nitrite inhibition on the anammox process. *Water Res.* **2012**, *46*, 2559–2569.

(45) Wunderlin, P.; Siegrist, H.; Joss, A. Online N_2O measurement: The next standard for controlling biological ammonia oxidation? *Environ. Sci. Technol.* **2013**, *47*, 9567–9568.

(46) Ma, Y.-F.; Zhang, Y.; Zhang, J.-Y.; Chen, D.-W.; Zhu, Y.; Zheng, H.; Wang, S.-Y.; Jiang, C.-Y.; Zhao, G.-P.; Liu, S.-J. The complete genome of *Comamonas testosteroni* reveals its genetic adaptations to changing environments. *Appl. Environ. Microbiol.* **2009**, *75*, 6812–6819.

(47) Horinouchi, M.; Hayashi, T.; Yamamoto, T.; Kudo, T. A new bacterial steroid degradation gene cluster in *Comamonas testosteroni* TA441 which consists of aromatic-compound degradation genes for seco-steroids and 3-ketosteroid dehydrogenase genes. *Appl. Environ. Microbiol.* **2003**, *69*, 4421–4430.

(48) Nishino, S. F.; Spain, J. C. Oxidative pathway for the biodegradation of nitrobenzene by *Comamonas* sp. strain JS765. *Appl. Environ. Microbiol.* **1995**, *61*, 2308–2313.

(49) He, Z.; Spain, J. C. Comparison of the downstream pathways for degradation of nitrobenzene by *Pseudomonas pseudoalcaligenes* JS45 (2-aminophenol pathway) and by *Comamonas* sp. JS765 (catechol pathway). *Arch. Microbiol.* **1999**, *175*, 309–316.

(50) Wu, J.; Jiang, C.; Wang, B.; Ma, Y.; Liu, Z.; Liu, S. Novel partial reductive pathway for 4-chloronitrobenzene and nitrobenzene degradation in *Comamonas* sp. strain CNB-1. *Appl. Environ. Microbiol.* **2006**, *72*, 1759–1765.

(51) Boon, N.; Goris, J.; Vos, P.; De Verstraete, W.; Top, E. M. Bioaugmentation of activated sludge by an indigenous 3-chloroaniline-degrading *Comamonas testosteroni* strain, I2gfp. *Appl. Environ. Microbiol.* **2000**, *66*.

(52) Goyal, A. K.; Zylstra, G. J. Molecular cloning of novel genes for polycyclic aromatic hydrocarbon degradation from *Comamonas testosteroni* GZ39. *Appl. Environ. Microbiol.* **1996**, *62*, 230–236.